ENHANCEMENT IN THE FIRE RESISTANT EFFICIENCY OF EPOXY RESIN BY SYNERGISTIC EFFECT BETWEEN METAL-ORGANIC FRAMEWORKS AND POLYETHYLENEIMINE-MODIFIED AMMONIUM POLYPHOSPHATE

TĂNG CƯỜNG HIỆU QUẢ CHỐNG CHÁY CỦA NHỰA EPOXY NHỜ HIỆU ỨNG HIỆP ĐỒNG GIỮA VẬT LIỆU KHUNG HỮU CƠ - KIM LOẠI VÀ AMMONIUM POLYPHOSPHATE ĐƯỢC BIẾN TÍNH BẰNG POLYETHYLENEIMINE

Nguyen Hong Tham[1], Nhung Hac Thi[1,3], Truong Cong Doanh[2], Tran Duc Long[4], Ho Thi Oanh[1], Tien Dat Doan[1,3], Nguyen Duc Tuy en[1], Minh-Tan Vu[2], Mai Ha Hoang[1,3,*]

DOI: https://doi.org/10.57001/huih5804.2025.298

ABSTRACT

Two metal-organic frameworks (MOFs), including ZIF-67 and ZIF-8, were successfully synthesized through self-assembly of organic bridging ligands and transition metal ions. Additionally, the MOFs were introduced into an intumescent flame-retardant epoxy composite containing polyethyleneimine-modified ammonium polyphosphate (APP@PEI). The synergistic effects between MOFs and APP@PEI on the flame retardancy and thermal stability of the epoxy matrix were found. Specially, the incorporation of ZIF-8 provied a superior enhancement in the fire resistance of the composite. The nanocomposite loading 3 wt% ZIF-8 and 7 wt% APP@PEI passed a V-0 rating in the UL-94 vertical burning test with a limiting oxygen index value of 30.3%. The formation of thermally stable metal phosphate compounds played a crucial role in improving the condensed-phase flame retardant efficiency of the nanocomposites, which reinforced the surface structure of the char layer to become more continuous and compact. Moreover, tensile and impact tests revealed that the presence of MOFs significantly improved the mechanical properties of the composite containing APP@PEI. This combination offered a promising approach for developing high-performance intumescent flame-retardant epoxy materials.

Keywords: *Metal-organic framework, intumescent flame retardants, epoxy, flame retardancy, synergistic effect.*

TÓM TẮT

Hai vật liệu khung kim loại- hữu cơ (MOFs) đã được tổng hợp thành công thông qua quá trình tự lắp ráp giữa các phối tử hữu cơ và ion kim loại chuyển tiếp. Sau đó, các MOFs này đã được thêm vào hệ compozit epoxy chứa amoni polyphosphate đã được biến tính bằng polyethyleneimine (APP@PEI). Tổ hợp MOFs và APP@PEI đã thể hiện hiệu ứng hiệp đồng rõ rệt trong việc nâng cao khả năng chống cháy và độ ổn định nhiệt của nền epoxy. Đặc biệt, sự kết hợp với ZIF-8 cho thấy sự cải thiện vượt trội hơn về khả năng chống cháy của vật liệu compozit. Nanocompozit chứa 3 wt% ZIF-8 và 7 wt% APP@PEI đạt phân loại V-0 trong thử nghiệm cháy đứng UL-94, đồng thời đạt giá trị chỉ số oxy giới hạn cao là 30,3%. Sự hình thành các hợp chất phosphate kim loại có độ bền nhiệt cao trong quá trình cháy đóng vai trò quan trọng trong việc gia cường cấu trúc lớp than trở nên bền chắc hơn, từ đó nâng cao hiệu quả chống cháy pha rắn của nanocompozit. Ngoài ra, sự có mặt của các vật liệu MOFs còn góp phần cải thiện đáng kể độ bền kéo và độ bền va đập compozit chứa APP@PEI. Sự kết hợp này mang đến một hướng tiếp cận đầy triển vọng để phát triển các vật liệu epoxy chống cháy.

Từ khóa: *Vật liệu khung hữu cơ - kim loại, chất chống cháy trương nở, epoxy, chống cháy, hiệu ứng hiệp đồng.*

[1]Institute of Chemistry, Vietnam Academy of Science and Technology, Vietnam
[2]Hanoi University of Industry, Vietnam
[3]Graduate University of Science and Technology, Vietnam Academy of Science and Technology, Vietnam
[4]Hanoi National University of Education, Vietnam
[*]Email: hoangmaiha@ich.vast.vn
Received: 26/5/2025
Revised: 22/7/2025
Accepted: 28/7/2025

1. INTRODUCTION

Epoxy resin (EP), a thermosetting polymer, has attracted considerable over the past decades due to its excellent solvent resistance, high mechanical strength, strong adhesion, outstanding electrical insulation, low shrinkage, ease of processing, and cost-effectiveness. As a result, EP is extensively utilized in various applications, such as electronic, electrical materials, adhesives, coatings, and fiber-reinforced composites [1-3]. However, its inherent high flammability and smoke emission significantly limit its use in high-performance materials [4]. Therefore, enhancing the flame retardancy and smoke suppression properties of epoxy resins is of great practical importance for broadening their application scope.

Intumescent flame retardants (IFRs) represent a class of halogen-free flame-retardant additives recognized for their favorable characteristics, including low toxicity, minimal smoke generation, and effective anti-dripping behavior [5]. Typically, IFRs are composed of three key components: acid, carbon, and gas source [6]. Upon thermal exposure, IFRs promote the formation an intumescent char layer, which serves as an insulating barrier and prevents oxygen penetration, effectively protecting the underlying polymer matrices from flame. Ammonium polyphosphate (APP) is widely employed as the acid component due to its phosphorus content and its ability to facilitate char formation in conjunction with other ingredients, thus significantly improving flame retardancy [6-8]. However, APP frequently exhibits poor compatibility and dispersibility with polymer matrices, which can adversely impact the mechanical properties of polymers and degrade their performance in engineering applications. To address these limitations, recent research has focused on modifying APP, particularly through surface functionalization with branched polyethyleneimine (APP@PEI) - a curing agent commonly used in thermosetting systems- to enhance its distribution and interaction within epoxy matrices [9, 10]. This approach has proven to be an efficient strategy for improving the flame-retardant performance of epoxy resins.

Meta-organic frameworks (MOFs), as a promising class of porous materials that have garnered significant attention across various fields, including gas separation, gas storage, chemical sensing, catalysis, proton conduction, batteries, and drug delivery, owing to stable porous structure, large surface areas, and adjustable pore size [11-14]. The organic ligands within the structure of MOFs not only enhance compatibility but also provide flame-retardant elements or groups, such as nitrogen-containing groups and aromatic structures [15]. Moreover, transition metal oxides produced during the thermal decomposition of MOFs present a catalytic effect, which promotes char formation and reduces smoke generation [16]. Consequently, MOFs have emerged as promising flame retardant additives for enhancing the fire resistance of polymer materials and represent a compelling alternative to conventional nanoparticles in flame-retardant applications. Recent studies have demonstrated that various existing MOFs, including ZIF-8, ZIF-67, and UiO-66, can be directly employed as flame retardants in polymer matrices. For instance, Zheng et al. [17] have reported that incorporating 2 wt% of Co-MOF, Zn-MOF, or Fe-MOF into epoxy resin effectively reduced the thermal degradation rate and increased char yield. Notably, the peak heat release rate (PHRR) of EP/Co-MOF, EP/Zn-MOF, and EP/Fe-MOF composites decreased from 866kW/m² to 595, 625, and 705kW/m², respectively-corresponding to reductions of 31.3%, 27.8%, and 18.6% compared to neat epoxy. However, the ligands comprising in these MOFs, such as 1, 4-benzenedicarboxylate acid and imidazole, do not contain flame retardant element or contain very low content of flame-retardant element [18]. Consequently, further enhancement of the flame-retardant performance of these MOFs is necessary. MOFs can be combined with various conventional flame retardant additives to form a synergistic flame-retardant system that enhance overall fire resistance. Recently, several studies been reported the combination between traditional flame retardants and MOFs. Liu et al. [19] developed a novel flame retardant (dZIF-8) by functionalizing ZIF-8 with derivatives of 9,10-dihydro-9-oxa-10-phosphaphenanthrene-10-oxide (DMZ). Combustion testing revealed that dZIF-8 effectively reduced the flammable property of epoxy resin. EP containing 2 wt% dZIF-8 exhibited excellent flame retardancy, achieving a high limiting oxygen index (LOI) value of 27.3%. Moreover, this formulation achieved a UL-94 V-1 rating, while EP composites containing 2 wt% DMZ or ZIF-8 alone failed to meet any classification. In another study, Wan et al. [20] synthesized a multi-layered core-shell flame retardant (APP-PEI@MXene@ZIF-67) and introduced into thermoplastic polyurethane (TPU). Compared to pure TPU, the composite containing 20 wt% of this hybrid additive showed a significant reduction in both heat and smoke release during combustion.

In this paper, transition metal-organic frameworks (ZIF-67 and ZIF-8) were synthesized by a straightforward method. Next, the MOFs was combined with APP@PEI as flame retardant fillers for EP. The flame retardancy, thermo-oxidative stability, and mechanical properties of these nanocomposites were investigated by the UL-94 vertical burning, limiting oxygen index test, thermal gravimetric analysis, tensile, and unnotched Izod impact measurements.

2. MATERIALS AND METHODS

2.1. Material

Cobalt (II) nitrate hexahydrate ($Co(NO_3)_2.6H_2O$, ACS reagent, ≥ 98%), zinc nitrate hexahydrate ($Zn(NO_3)_2.6H_2O$, 98%), 2-methylimidazole (2-mIm, 99%), branched polyethyleneimine (PEI, 99%, M.W.300), methanol (> 99.9%) were purchased from Sigma- Aldrich. Epoxy resin (GELR128, density: 1.16 - 1.20gcm^{-3}, viscosity: 11000 - 15000mPas, epoxy equivalent: 184 - 190g/equivalent, epoxy value: 0.58 - 0.64 equivalent/100g), and hardener RICH6328 (density: 0.99gcm^{-3}, viscosity: 250 - 450cps, amine value: 300mg KOH/g) were bought from Guangzhou Rich Chemical Co., Ltd, China. Commercial APP (form II) was supplied by China. High-purity absolute ethanol was used directly without additional purification.

2.2. Synthesis of ZIF-67 and ZIF-8

2.2.1. Synthesis of ZIF-67

ZIF-67 was synthesized according to a previously reported method [21]. Briefly, 14.55g of $Co(NO_3)_2{\cdot}6H_2O$ was dissolved in 500mL of methanol. Simultaneously, 16.42g of 2-mIm was also dissolved in another 500mL of methanol. The two solutions were then mixed under stirring for 15 min. Afterward, the reaction mixture was kept static at room temperature for 24h. Next, the resulting solid was obtained by centrifugation at 10000rpm and washed many times with ethanol. Finally, the product was dried at 80°C for 24h and ground into a fine purple powder, referred to as ZIF-67.

2.2.2. Synthesis of ZIF-8

The synthesis of ZIF-8 was primarily carried out in two steps [22]. First, 14.55g of $Zn(NO_3)_2.6H_2O$ was dissolved in 500mL of methanol. At the same time, 32.84g of 2-methylimidazole was dissolved in another 500mL of methanol. Then, two solutions were mixed under stirring for 15 min. Next, the reaction mixture was kept static at room temperature for 24h. Finally, the obtained solid was collected by centrifugation at 12000rpm and washed several times with ethanol. Finally, the product was dried at 80°C for 24 h to obtain ZIF-8 as a white powder.

2.2.3. Preparation of APP@PEI

Ammonium polyphosphate was modified with polyethyleneimine (APP@PEI) based on previous literature [23]. The preparation process of APP@PEI was carried out as follows: First, a solvent mixture was prepared by combining 210mL of ethanol and 10 mL of distilled water. Then, 3.5g of PEI was completely dissolved in 20mL of this solvent mixture under N_2 atmosphere. Meanwhile, 10g of APP and 200mL of the solvent mixture were added to a three-neck flask, stirred, and heated to 90°C under N_2 atmosphere. Afterwards, the PEI solution was introduced into the flask, and the reaction system was continuously stirred at 90°C for 2h under N_2 atmosphere. The resulting white solid was then filtered and washed several times with ethanol to eliminate excess PEI. Finally, the sample was dried overnight in a vacuum oven at 80°C to obtain APP@PEI powder.

2.2.4. Preparation of flame retardant epoxy nanocomposites

The EP composites were prepared through a traditional curing process, with a hardener to epoxy resin mass ratio of 1:1. The preparation process consisted of the following steps: a specific amount of the flame retardant additives was dispersed in the hardener through stirring and ultrasonic treatment. Subsequently, EP resin was incorporated into the blend with gentle stirring. Once the mixture became homogeneous, it was poured into a silicone mold prepared according to the standard measurement's dimensions. After curing at room temperature for 24h and then at 60°C for 12h, the EP composites were investigated the flame retardancy, thermal stability, and mechanical properties. The composite formulations are provided in Table 1.

Table 1. Composition for each of the prepared composite formulations based on epoxy

Sample	Composition (wt.%)			
	EP	APP@PEI	ZIF-67	ZIF-8
EP	100	-	-	-
10IFR/EP	90	10	-	-
3ZIF-67/7IFR/EP	90	7	3	-
3ZIF-8/7IFR/EP	90	7	-	3

Abbreviations: *IFR (APP@PEI).*

2.3. Characterizations

X-ray diffraction (XRD) data were performed on a D8 Advance diffractometer (Brucker, Germany) using Cu Kα

radiation (λ = 1.5406Å) source in a 2θ range from 10° to 70°. Fourier transform infrared (FT-IR) spectra were acquired from on a L1600400 Spectrum two DTGS spectrometer (PerkinElmer, USA) in a range of 450 - 4000cm^{-1}. Scanning electron microscopy (FE-SEM) (S-4800, Hitachi, Japan) with an accelerating voltage of 3kV and 5kV was used to observe the morphology of synthesized MOFs and investigate the microstructures of the char residues, respectively. Thermogravimetric analysis (TGA) was performed on a LABSYS Evo STA analyzer (Setaram, France) at a heating rate of 10°C min^{-1} under an air atmosphere from 50 to 900°C.

UL-94 vertical combustion test (UL94-V) was carried on a GT-MC35F-2 horizontal and vertical flame chamber (Gester, China) based on ASTM D3801. Limiting oxygen index (LOI) values were determined by using a Yasuda 214 oxygen index flammability tester (Japan) following ASTM D2863-13. The sizes of samples for both measurements were 125mm × 13mm × 3.2mm.

Tension properties of epoxy composites were determined according to ISO 527 using a AI-7000M Testing Machine (Gotech, Taiwan) at a tensile rate of 20mmmin^{-1}. The tested specimens had dumbbell-shaped with a Gauge length of 50 mm. Unnotched Izod impact strength of the materials were measured following ASTM D4812 using mechanical test equipment (Test Resources, USA). The samples had a dimension of 64mm × 13mm × 3mm. The results for each formulation represented an average of five measurements, accompanied by error values.

3. RESULTS AND DISCUSSION

3.1. Characterization of MOFs

FT-IR spectra of the as-synthesized ZIF-67 and ZIF-8 samples are shown in Figure 1(a, c). In the case of ZIF-67, the absorption peaks at 3131 and 2925cm^{-1} assigns to the C–H vibrations in the aromatic ring and the aliphatic chain of the 2-methylimidazole bridge. The peak at 1579cm^{-1} corresponds to the C=N stretching vibrations. The bands observed in the range of 1418 - 993cm^{-1} are characteristic of C–N vibrations [24]. Additionally, the presence of an absorption peak at 425cm^{-1} indicates of the formation of the Co-N bond [25]. Due to the use of the same ligand in the fabrication process, the FT-IR spectra of ZIF-8 exhibits similar characteristic peaks compared to ZIF-67. On the other hand, a new peak at 418cm^{-1} assigned to Zn–N stretching vibrations appear in the FT-IR spectrum of ZIF-8. These results agree well with the previous work [22].

The crystal structures of the obtained samples can be studied by X-ray diffraction (XRD). In term of ZIF-67 (Figure 1b), the characteristic diffraction peaks presenting at 2θ ~ 7.3°, 10.4°, 12.7°, 14.8°, 16.5°, 18.0°, 22.1°, 24.4°, 25.6° and 26.7° correspond to (011), (002), (112), (022), (013), (222), (114), (233), (244), and (134) planes, respectively, which is in good agreement with ZIF-67 topology [26, 27]. No identifiable peaks from impurities or precursor compounds are observed, indicating the high purity of the synthesized samples. As for ZIF-8 (Figure 1d), sharp diffraction peaks which are similar to those of ZIF-67 are shown in the XRD pattern [28].

The morphology of the obtained nanomaterials was observed by FE-SEM imaging. As shown in Figure 2, both ZIF-67 and ZIF-8 exhibit high crystallinity with well-defined rhombic dodecahedral structures and uniform particle size distributions. However, a significant difference in particle size between two nanomaterials is observed. Specifically, ZIF-8 particles are approximately 60nm in size, markedly smaller than those of ZIF-67, which are around 300nm.

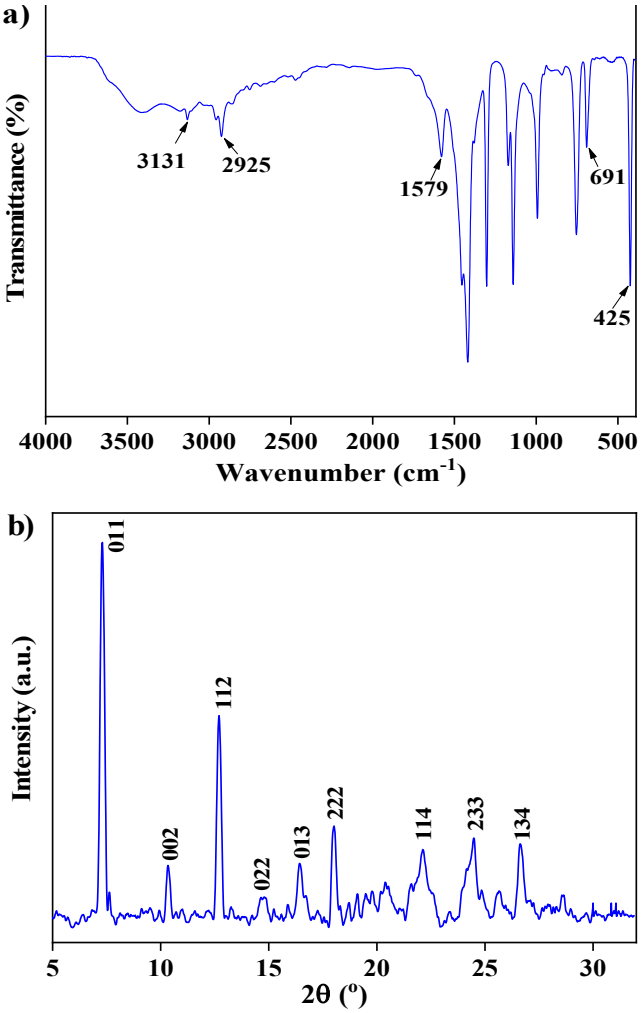

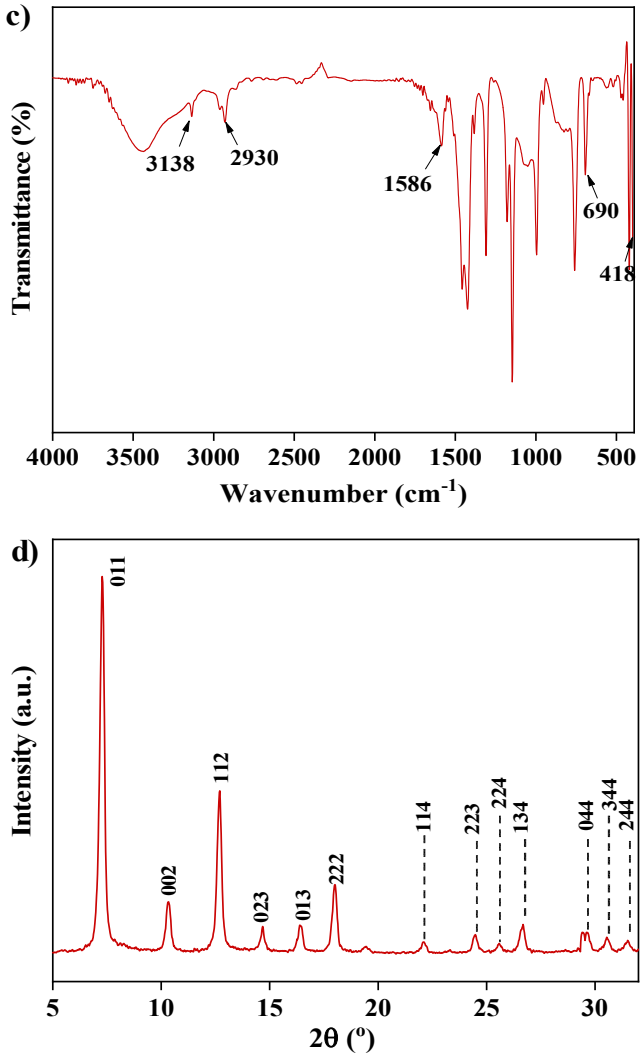

Figure 1. FT-IR spectra and XRD patterns of the synthesized ZIF-67 (a, b) and ZIF-8 (c, d)

Thermal properties of the as-synthesized MOFs were investigated by thermogravimetric analysis under an air atmosphere, with the corresponding TGA and DTG curves shown in Figure 3. For ZIF-67, the initial mass loss below 250°C is attributed to the removal of guest molecules (e.g., solvent) and gas molecules adsorbed on the material surface, while the major decomposition between 250 - 550°C correspond to the breakdown of the organic linkers and the collapse of the framework [29]. The char yield of ZIF-67 at 900°C is 34.83 wt.%. In the case of ZIF-8, the substantial decomposition primarily takes place between 300 and 700°C, during which the organic linkages degrade, leading to the collapse of the framework structure [30]. Notably, the T_{max} value of ZIF-8 is 462.03°C, which is 20.6°C higher than that of ZIF-67. Additionally, the residual yield of ZIF-8 increases by 7.67% compared to ZIF-67.

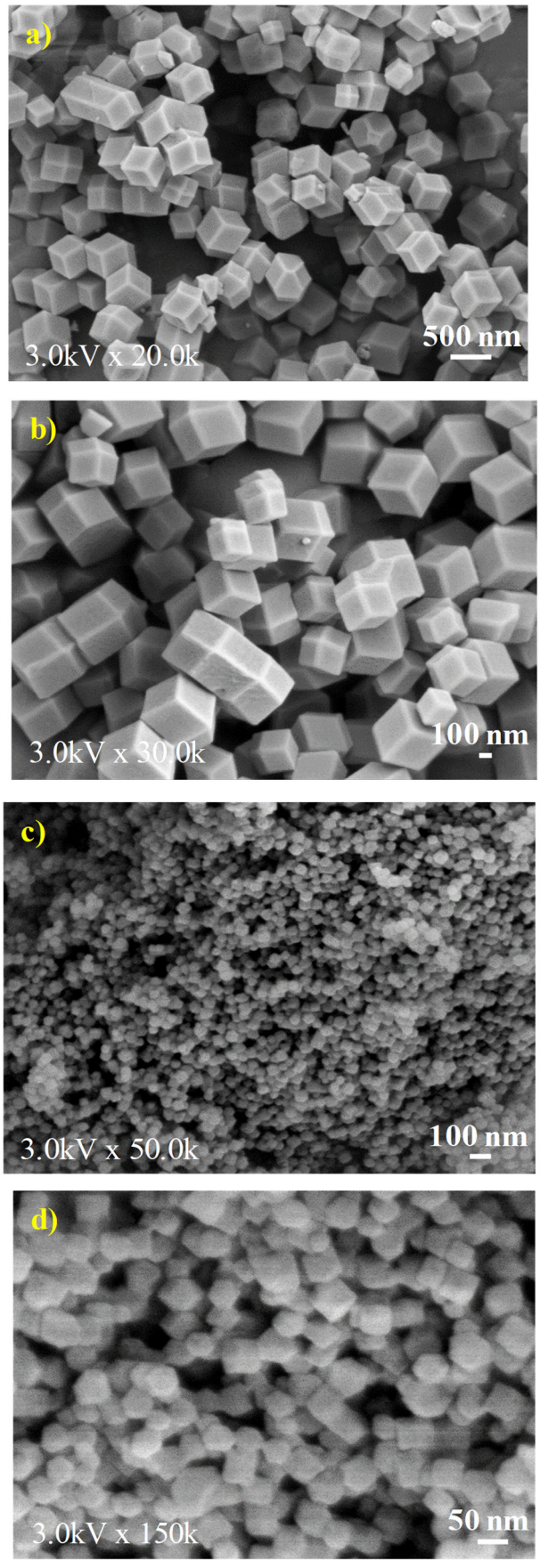

Figure 2. SEM images of the synthesized ZIF-67 (a, b) and ZIF-8 (c, d)

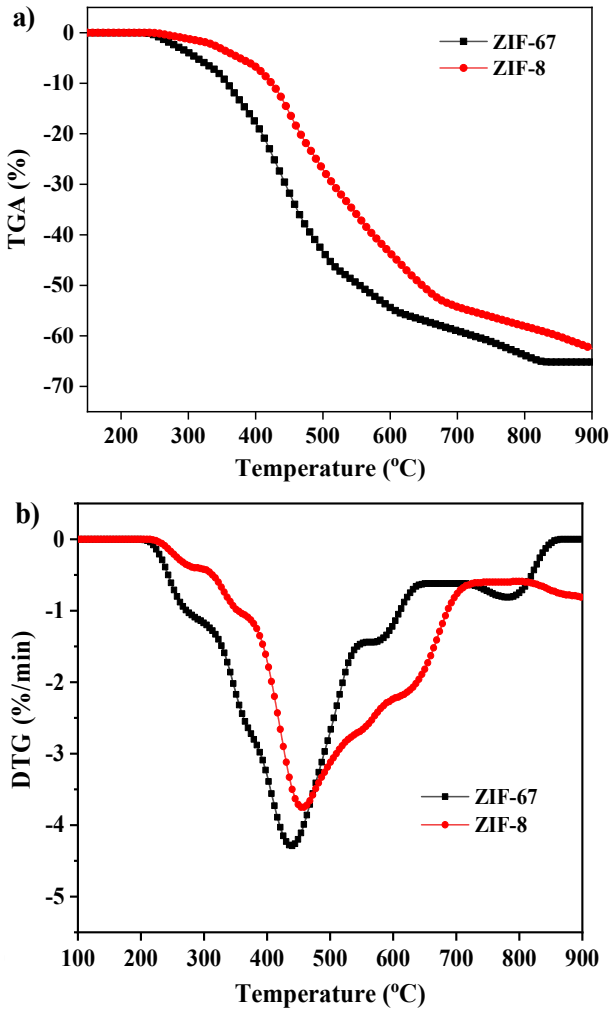

Figure 3. TGA (a) and DTG (b) curves of the synthesized MOFs under air atmosphere

3.2. Flame retardancy

The flame retardancy of EP and its composites was evaluated using UL94-V and LOI tests, with the results are summarized in Table 2. It is evident that pure EP is highly flammable, burning completely after the first ignition during the UL94-V test. The incorporation of 10 wt.% APP@PEI significantly improved the fire resistance of the epoxy resin, increasing the LOI value from 20.2% to 25.9%. However, this composite still fails to achieve a UL-94 rating, suggesting that further formulation optimization is necessary. Therefore, the effect of the combination between APP@PEI and a small amount of MOFs on the flame retardancy of EP was investigated. The replacement of 3 wt.% APP@PEI with ZIF-67 or ZIF-8 significantly enhances the flame retardancy of the composite. This result can be explained due to the synergistic flame-retardant effect between APP@PEI and MOFs. Among them, the 3ZIF-8/7IFR/EP nanocomposite exhibits a superior flame retardancy with short self-extinguishing times in the UL-94 V test (t_1 = 1.6s and t_2 = 2.7s) and a high LOI value of 30.3%.

Table 2. Flame retardancy and mechanical properties of epoxy resin and its composites

Samples	UL94-V (3.2 mm)			LOI (%)	Tensile strength (MPa)	Impact strength (KJ/m^2)
	Rating	t_1[a] (s)	t_2[b] (s)			
EP	NR[c]	Burnt out	-	20.2	68.23 ± 0.2	31.80 ± 0.1
10IFR/EP	NR	2.1	58	25.9	47.85 ± 0.6	9.70 ± 0.3
3ZIF-67/7IFR/EP	V-0	2.6	4.3	29.8	53.46 ± 0.7	10.70 ± 0.6
3ZIF-8/7IFR/EP	V-0	1.6	2.7	30.3	66.15 ± 0.3	11.32 ± 0.2

Abbreviations: *[a]t_1: Self-extinguishing time after the first ignition; [b]t_2: Self-extinguishing time after the second ignition; [c]NR: No rating.*

3.3. Thermal oxidative behaviour

The thermal behavior of EP and its composite were analyzed by TGA under air atmosphere. The TGA and DTG curve are presented in Figure 4, and the corresponding data is summarized in Table 3. The EP resin undergoes two distinct degradation stages [31], leaving an exceptionally low residual char of approximately 0.59 wt% at 900°C. For 10IFR/EP composite, the T_{max} value reduces by 37.39°C compared to the EP sample, whereas the char yield increases significantly. These results can be explained due to the breakdown of APP, which releases phosphoric and polyphosphoric acids. These acids catalyse dehydration and carbonization of the epoxy matrix, promoting the formation of an intumescent char layer that acts as a protect barrier and effectively insulates the underlying material from heat and flame [23]. The partial replacement of APP@PEI with ZIF-67 and ZIF-8 significantly improves the thermal oxidative stability of the composite. Specifically, the T_{max} value of 3ZIF-67/7IFR/EP and 3ZIF-8/7IFR/EP are elevated by 12.41°C and 25.95°C, respectively, in comparison with the 10IFR/EP composite. Furthermore, the char yield at 900°C for these nanocomposites increased substantially, reaching 13.22% and 14.85% at 900°C. These improvements are attributed to the presence of metal oxides (Co_3O_4 and ZnO) from the degradation of the MOF structures, catalyzing for the char formation of the composite. Moreover, the synergistic interaction between APP@PEI and the metal oxides can produce highly thermally stable metal phosphate compounds, reinforcing the char layer surface of the nanocomposites. As a result, the thermal decomposition rate of the

nanocomposites is significantly reduced. These findings explain the enhanced flame retardancy of the nanocomposites compared to the 10IFR/EP composite.

Table 3. TGA data of EP and its composites under air atmosphere

Sample	T_{onset}[a] (°C)	T_{max}[b] (°C)	Residue at 900°C (wt%)
EP	284.10	373.29	0.59
10IFR/EP	307.50	335.90	7.92
3ZIF-67/7IFR/EP	308.81	348.31	13.22
3ZIF-8/7IFR/EP	308.39	361.85	14.85

Abbreviations: *[a]T_{onset}: Temperature at 5% weight loss; [b]T_{max}: Temperature at maximum weight loss rate*

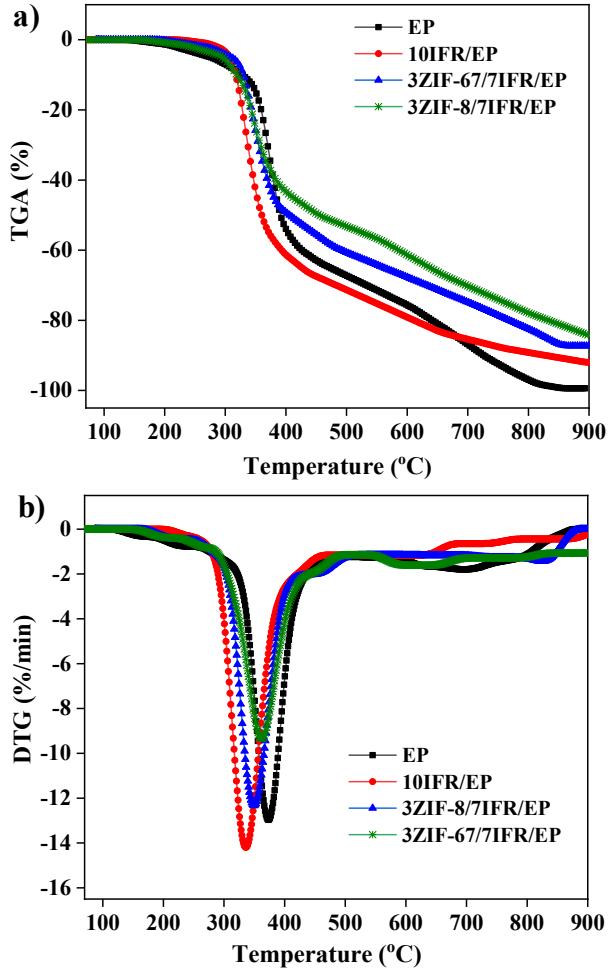

Figure 4. TGA (a) and DTG (b) curves of EP and its composites under air atmosphere

3.4. Flame-retardant mechanism

The formation of a stable and compact char layer plays a pivotal role in enhancing the flame retardancy of burning materials. Therefore, the analysis of the char residues is critical for elucidating the combustion behavior and flame-retardant mechanism of polymer composites. In order to investigate the synergistic effect between APP@PEI and MOFs, the samples EP and its composites were calcined to 900°C at rate of 10°C/min, using samples of the same weight. Figure 5 shows digital photographs of EP and its composites after calcination.

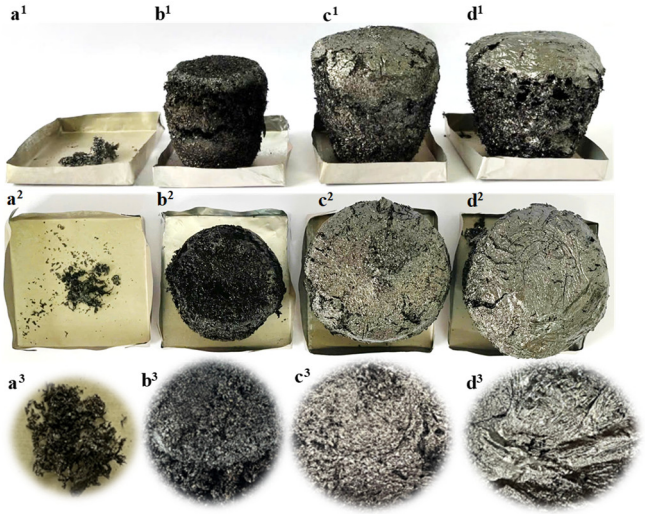

Figure 5. Digital photographs of char residue for EP and its composites after calcination at 900°C: EP (a); 10IFR/EP (b); 3ZIF-67/7IFR/EP (c) và 3ZIF-8/7IFR/EP (d). Index 1 illustrates the frontal view, indexes 2 and 3 indicate the top view

As shown in Figure 5a (a^1, a^2, a^3), the EP sample demonstrates a minimal char yield, which is consistent with the TGA results. In contrast, the addition of 10 wt.% APP@PEI significantly promotes char formation, resulting in a thick and porous char layer (Figure 5b (b^1-b^3)). However, this char structure is relatively soft and easily damaged, which may compromise its effectiveness as a protective barrier during combustion. Compared to the 10IFR/EP composite, the intumescence of the nanocomposites containing ZIF-67 and ZIF-8 increases notably, and their char surfaces become more continuous and compact (Figure 5c and d). This observation accounts for the improvement in the flame-retardant efficiency of the nanocomposites compared to the composites containing only APP@PEI. In the nanocomposites, fewer cracks are observed on the char surface of 3ZIF-8/7IFR/EP, which markedly contributes to its superior flame-retardant performance compared to 3ZIF-67/7IFR/EP.

Additionally, the chemical composition of char residues was investigated by FT-IR spectroscopy (Figure 6). Characteristic peaks at 2926 and 2854cm^{-1} (-CH_2 stretching), 1744cm^{-1} (C=O stretching), and 1625cm^{-1} (C=C stretching) are observed across all spectra [17, 32, 33]. This result indicates that aromatization and carbonization processes occur during the thermal

decomposition of the composites, facilitating the formation of a stable and thermally insulating char layer. In addition, an absorption band at about 1024cm^{-1}, corresponding to P-O stretching, appears in the FT-IR spectrum of the 10IFR/EP residue [34], suggesting the development of a phosphorus-rich char structure. For 3ZIF-67/7IFR/EP, an increase in the intensity of the peak at 1027cm^{-1} can be attributed to the overlap of P-O vibrations in the phosphorus-rich char layer and in the PO_4^{3-} groups of metal phosphates. Additionally, new peaks at 714 and 855cm^{-1}, asigned to P–O–P linkages of PO_4^{3-} groups, are detected [35]. In the case of 3ZIF-8/7IFR/EP, apart from the P-O vibrations in the phosphorus-rich char structure at 945cm^{-1}, a new absorption band at 947 - 1200cm^{-1} is observed, which attributes to stretching of PO_4^{3-} groups in metal phosphates [36]. These results indicate that, along with the phosphorus-rich char structure, highly thermally stable metal phosphate compounds are generated during combustion of the nanocomposites, resulting from the interaction between the decomposition products of APP and the metal-organic framework materials.

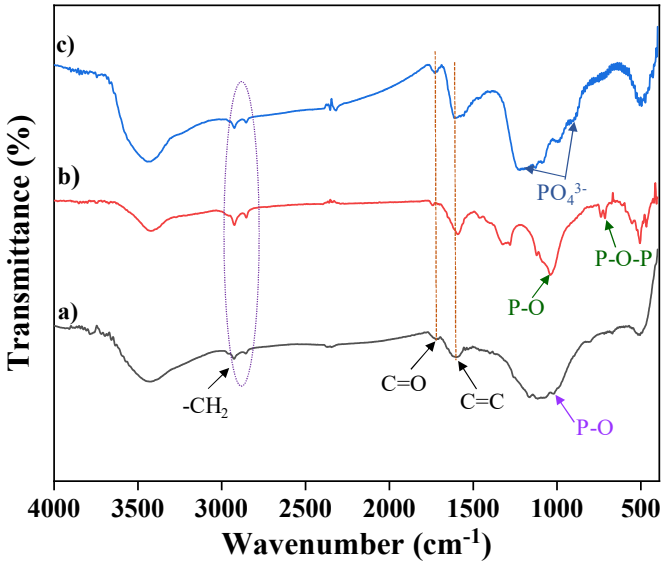

Figure 6. FT-IR spectra of char residues of 10IFR/EP (a), 3ZIF-67/7IFR/EP (b) và 3ZIF-8/7IFR/EP (c) after calcination at 900°C

Based on the above discussions and previous studies, the flame retardant mechanism of the nanocomposites 3ZIF-67/7IFR/EP and 3ZIF-8/7IFR/EP can be proposed as follows: At low temperature, APP, PEI, and hardener of EP begin to degrade, releasing NH_3 and H_2O. Simultaneously, ZIF-67 and ZIF-8 also undergoes the breakdown of the organic ligands, producing NH_3 and metal oxides, including Co_3O_4 and ZnO [37]. The released gases not only dilute oxygen and flammable decomposition products but also act as blowing agents that promote the expansion of the intumescent char layer. Subsequently, the decomposition of APP generates phosphoric acid and its poly-/ultra-/pyro-derivative. These derivatives promote dehydration, esterification, and aromatization reactions between EP matrix and APP, resulting in a phosphorus - rich aromatic structure. The presence of the metal oxides acts as a catalyst, accelerating the char formation process. Furthermore, part of phosphoric acid can react with Co_3O_4 and ZnO, forming highly thermally stable metal phosphates compounds. As the temperature increases, P-N-C structures are formed, but eventually decompose into non-combustible N-containing gases at higher temperatures [23], contributing to the flame inhibition in the gas phase. In constrast, aromatic ring structures containing P-O-P, C=C, and C=O bonds remain within the char residue, and the formation of metal phosphates helps to reinforce this char structure becoming more continuous and compact. Consequently, a robust and thermally stable char barrier is formed, inhibiting the heat transfer to the underlying material and restricting the diffusion of flammable gases into the combustion zone. Thus, the condensed-phase flame retardant mechanism of the nanocomposites exhibit higher effectiveness compared to the 10IFR/EP composite.

3.5. Mechanical properties

Yield tensile and unnotched Izod impact strengths of EP resin and its composites are presented in Table 3. The presence of APP@PEI negatively affects the mechanical properties of EP. In particular, the tensile and impact strengths of 10IFR/EP are decreased by 29.87% and 69.50%, respectively, compared to the neat EP resin. Although the compatibility of APP within the EP matrix improves after modification with PEI, clustering of the microparticles still occurs (Figure 7a). Moreover, the large particle size of this filler further contributes to the deterioration in mechanical properties. The substitution of APP@PEI with a small quantity of MOFs improves mechanical properties of the composite loading APP@PEI. Notably, the nanocomposite incorporating ZIF-8 demonstrates superior mechanical properties over the containing ZIF-67 counterpart. Specifically, the 3ZIF-8/7IFR/EP sample exhibits a tensile strength of 66.15MPa and an impact strength of 11.32kJ/m^2, representing increase of 23.74% and 5.8%, respectively, compared to the 3ZIF-67/7IFR/EP. These improvements can be

attributed to the particle size and the dispersion levels of MOFs within the the polymer matrix.

The dispersion and interfacial behaviour of MOF particles within the polymer matrix play a critical role in determining the mechanical properties of the resulting composites. Compared to ZIF-67, ZIF-8 exhibits a more homogeneous distribution throughout the EP matrix. Additionally, stronger interfacial adhesion is observed between ZIF-8 and the EP matrix, as evidenced by the reduced number of interfacial voids in Figure 7(d–f). The incorporation of ZIF-8 also mitigates the agglomeration of APP@PEI in the 3ZIF-8/7IFR/EP nanocomposite. In contrast, significant interfacial gaps are present in the 3ZIF-67/7IFR/EP system, as shown in Figure 7(b, c), indicating weaker interfacial bonding. This phenomenon is likely due to the bigger particle size of ZIF-67. Consequently, these structural differences explain the superior mechanical reinforcement effect observed in 3ZIF-8/7IFR/EP compared to 3ZIF-67/7IFR/EP.

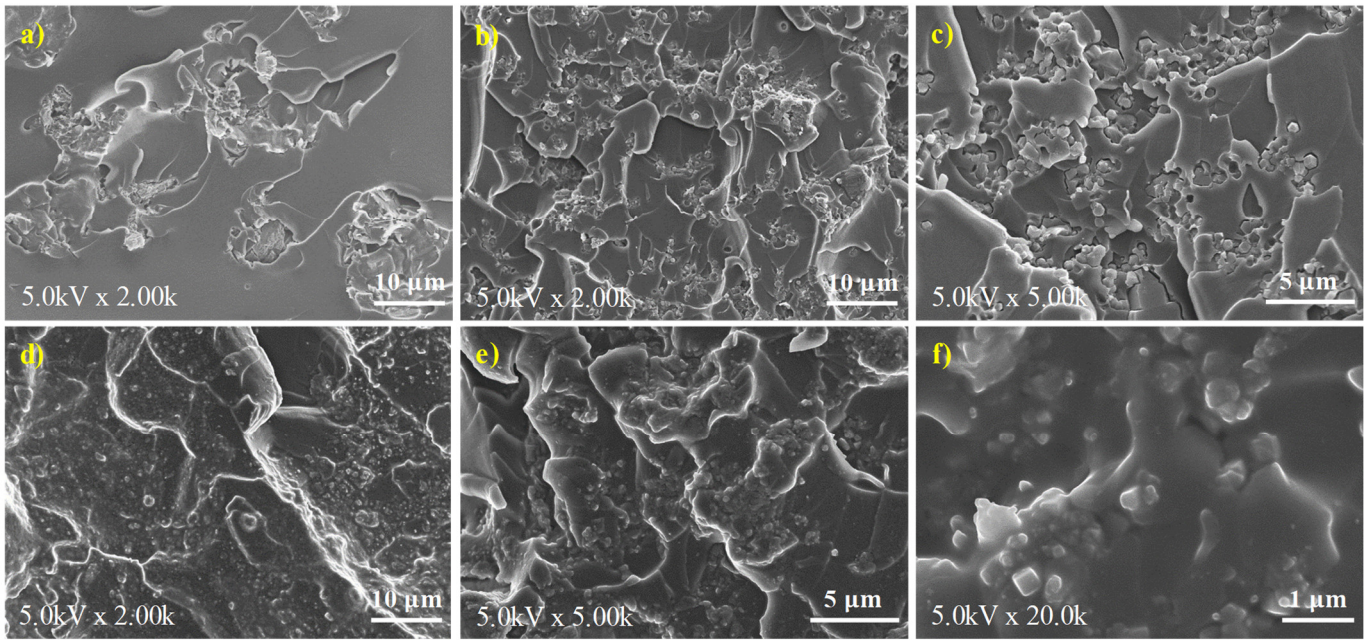

Figure 7. The fracture surface images of IFR/EP (a), 3ZIF-67/7IFR/EP (b, c) and 3ZIF-8/7IFR/EP (d, e, f) at different magnifications

4. CONCLUSION

In this study, two different types of MOFs, ZIF-67 and ZIF-8, were successfully synthesized using simple method. Their structure, morphology, and composition were measured by XRD, FTIR, TGA, and SEM. These MOFs were subsequently incorporated into an intumescent flame-retardant epoxy system to investigate their effect on thermal stability and flame retardancy. Both ZIF-67 and ZIF-8 exhibited excellent synergistic effects with APP@PEI on the flame retardancy and thermal stability. Notably, the 3ZIF-8/7IFR/EP nanocomposite achieved superior performance, including a UL-94 V-0 rating, a high LOI of 30.3%, and a char yield of 14.85 wt% at 900°C. The synergistic flame-retardant mechanism of the mixture of APP@PEI and MOFs was also discussed in both the condensed and gas phases. In the condensed phase, APP@PEI promoted the formation of a thermally stable, phosphorus-rich char layer during combustion, which acted as a physical barrier, protecting the underlying nanocomposite from flame. Furthermore, the interaction between decomposition products of MOFs and APP@PEI generated thermally stable metal phosphate compounds, contributing to a more continuous and compact char structure. In the gas phase, both MOFs and APP@PEI released non-combustible gases, such as NH_3, H_2O, and nitrogen-containing species. These gases acted not only as blowing agents for the intumescence of the char layer, but also as inert diluents to reduce oxygen concentration and flammable decomposition products. Moreover, the presence of MOFs significantly improved the tensile and impact strengths of the APP@PEI-loaded composite. The nanocomposite loading 3 wt% ZIF-8 and 5 wt% APP@PEI, with high flame retardant efficiency and good mechanical property, shows great potential for applications in fields with stringent fire safety requirements, including electronics, transportation, construction, and consumer goods. Future research should focus on optimizing MOF structures and

developing hybrid or functionally modified MOFs. Simultaneously, efforts should be directed toward enhancing scalable synthesis methods and thoroughly assessing the safety of decomposition products, aiming to enable more sustainable and effective real-world applications.

ACKNOWLEDGMENTS

This research is funded by Vietnam Academy of Science and Technology under grant number "KHCBHH.02/24-25".

REFERENCES

[1]. Song X., Q. Li, Z. Han, B. Hou, Y.T. Pan, Z. Geng, J. Zhang, L. Haurie Ibarra, R. Yang, "Synchronous modification of ZIF-67 with cyclomatrix polyphosphazene coating for efficient flame retardancy and mechanical reinforcement of epoxy resin," *Journal of Colloid And Interface Science*, 667, 223-236, 2024.

[2]. Song K., Y.T. Pan, J. Zhang, P. Song, J. He, D.Y. Wang, R. Yang, "Metal–Organic Frameworks–Based Flame-Retardant System for Epoxy Resin: A Review and Prospect," *Chemical Engineering Journal*, 468, 2023.

[3]. Niu H., G. Wu, X. Wang, H. Ding, Y. Hu, "Synthesis of a vanillin-derived bisDOPO co-curing agent rendering epoxy thermosets simultaneously improved flame retardancy, mechanical strength and transparency," *Polymer Degradation and Stability*, 211, 2023.

[4]. Song K., Y. Wang, F. Ruan, J. Liu, N. Li, X. Li, "Effects of a Macromolecule Spirocyclic Inflatable Flame Retardant on the Thermal and Flame Retardant Properties of Epoxy Resin," *Polymers (Basel),* 12(1), 2020.

[5]. Xu B., L. Shao, J. Wang, Y. Liu, L. Qian, "Enhancement of the intumescent flame retardant efficiency in polypropylene by synergistic charring effect of a hypophosphite/cyclotetrasiloxane bi-group compound," *Polymer Degradation and Stability,* 181, 2020.

[6]. Jin X., J. Zhang, Y. Zhu, A. Zhang, R. Wang, M. Cui, D.Y. Wang, X. Zhang, "Highly efficient metal-organic framework based intumescent poly(L-lactic acid) towards fire safety, ignition delay and UV resistance," *International Journal of Biological Macromolecules,* 250, 126127, 2023.

[7]. Khanal S., Y. Lu, S. Ahmed, M. Ali, S. Xu, "Synergistic effect of zeolite 4A on thermal, mechanical and flame retardant properties of intumescent flame retardant HDPE composites," *Polymer Testing*, 81, 2020.

[8]. Zheng P., H. Zhao, J. Li, F. Wu, Q. Liu, "Flame retardant based on metal catalyzed instantaneous crosslinking to form carbon for improving the safety performance of aircraft epoxy resin," *Safety Science*, 178, 2024.

[9]. Huang J., M. Gao, T. Pan, Y. Zhang, Y. Lin, "Effective thermal conductivity of epoxy matrix filled with poly(ethyleneimine) functionalized carbon nanotubes," *Composites Science and Technology,* 95, 16-20, 2014.

[10]. Guo Q., G. Li, P. Zhu, Z. Xu, T. Zhao, R. Sun, C. P. Wong, "Interfacial engineering of epoxy/silica nanocomposites by amino-rich polyethyleneimine towards simultaneously enhanced rheological and thermal-mechanical performance for electronic packaging application," *Composites Part B: Engineering,* 245, 2022.

[11]. Peng Y., Y. Li, Y. Ban, H. Jin, W. Jiao, X. Liu, W. Yang, "Membranes. Metal-organic framework nanosheets as building blocks for molecular sieving membranes," *Science,* 346(6215), 1356-9, 2014.

[12]. Xiao-Min Li, Y.W., Yongbiao Mu, Junkuo Gao, Lin Zeng, "Oriented Construction of Efficient Intrinsic Proton Transport in MOF-808 Metal-Organic Framework," *Journal of Materials Chemistry A*, 10, 18592-18597, 2022.

[13]. Ye Z., Y. Jiang, L. Li, F. Wu and R. Chen, "Rational Design of MOF-Based Materials for Next-Generation Rechargeable Batteries," *Nano-Micro Letters,* 13(1), 203, 2021.

[14]. Ma D., G. Wang, J. Lu, X. Zeng, Y. Cheng, Z. Zhang, N. Lin, Q. Chen, "Multifunctional nano MOF drug delivery platform in combination therapy," *European Journal of Medicinal Chemistry*, 261, 115884, 2023.

[15]. Hou Y., W. Hu, Z. Gui, Y. Hu, "Preparation of Metal–Organic Frameworks and Their Application as Flame Retardants for Polystyrene," *Industrial & Engineering Chemistry Research,* 56(8), 2036-2045, 2017.

[16]. Zhou K., R. Gao, X. Qian, "Self-assembly of exfoliated molybdenum disulfide (MoS(2)) nanosheets and layered double hydroxide (LDH): Towards reducing fire hazards of epoxy," *Journal of Hazardous Materials,* 338, 343-355, 2017.

[17]. Zheng Y., Y. Lu, K. Zhou, "A novel exploration of metal–organic frameworks in flame-retardant epoxy composites," *Journal of Thermal Analysis and Calorimetry,* 138(2), 905-914, 2019.

[18]. Zhang G., Y. Dong, M. Yao, Y. Cui, W. Meng, S. Wang, H. Qu, J. Xu, "Preparation of a MOF flame retardant containing phosphazene ring and its effect on the flame retardant of epoxy resin," *Reactive and Functional Polymers*, 191, 2023.

[19]. Liu D., Y. Cui, T. Zhang, W. Zhao, P. Ji, "Improving the flame retardancy and smoke suppression of epoxy resins by introducing of DOPO derivative functionalized ZIF-8," *Polymer Degradation and Stability,* 194, 2021.

[20]. Wan M., C. Shi, L. Chen, L. Deng, Y. Qin, H. Che, J. Jing, J. Li, X. Qian, "Core-shell flame retardant/APP-PEI@MXene@ZIF-67: A nanomaterials self-assembly strategy towards reducing fire hazard of thermoplastic polyurethane," *Polymer Degradation and Stability,* 226, 2024.

[21]. Li Q., Z. Han, X. Song, Y.T. Pan, Z. Geng, H. Vahabi, V. Realinho, R. Yang, "Enhancing char formation of flame retardant epoxy composites: Onigiri-like ZIF-67 modification with carboxymethyl beta-cyclodextrin crosslinking," *Carbohydrate Polymers,* 333, 121980, 2024.

[22]. Wang G., W. Xu, R. Chen, W. Li, Y. Liu, K. Yang, "Synergistic effect between zeolitic imidazolate framework-8 and expandable graphite to improve the flame retardancy and smoke suppression of polyurethane elastomer," *Journal of Applied Polymer Science,* 137(1), 2019.

[23]. Tan Y., Z.B. Shao, L.X. Yu, Y.J. Xu, W.H. Rao, L. Chen, Y.Z. Wang, "Polyethyleneimine modified ammonium polyphosphate toward polyamine-

hardener for epoxy resin: Thermal stability, flame retardance and smoke suppression," *Polymer Degradation and Stability*, 131, 62-70, 2016.

[24]. Saeed S., R. Bashir, S.U. Rehman, M.T. Nazir, A.L. ZA, A. Muteb Aljuwayid, A. Abid, A. Adnan, "Synthesis and Characterization of ZIF-67 Mixed Matrix Nanobiocatalysis for CO(2) Adsorption Performance," *Frontiers in Bioengineering and Biotechnology*, 10, 891549, 2022.

[25]. Wang Q., Z. Zhang, S. Shi, F. Wu, Z. Zhang, G. Li, Y. Suo, "Highly active cobalt- and nitrogen-doped carbon derived from ZIF-67@melamine towards oxygen reduction reaction," *Journal of Electroanalytical Chemistry*, 894, 2021.

[26]. Guo X., T. Xing, Y. Lou, J. Chen, "Controlling ZIF-67 crystals formation through various cobalt sources in aqueous solution," *Journal of Solid State Chemistry*, 235, 107-112, 2016.

[27]. Qin J., S. Wang, X. Wang, "Visible-light reduction CO 2 with dodecahedral zeolitic imidazolate framework ZIF-67 as an efficient co-catalyst," *Applied Catalysis B: Environmental,* 209, 476-482, 2017.

[28]. Xu W., G. Wang, Y. Liu, R. Chen, W. Li, "Zeolitic imidazolate framework-8 was coated with silica and investigated as a flame retardant to improve the flame retardancy and smoke suppression of epoxy resin," *RSC Advances*, 8(5), 2575-2585, 2018.

[29]. Lin K.Y., H.A. Chang, "Ultra-high adsorption capacity of zeolitic imidazole framework-67 (ZIF-67) for removal of malachite green from water," *Chemosphere,* 139, 624-31, 2015.

[30]. Schejn A., L. Balan, V. Falk, L. Aranda, G. Medjahdi, R. Schneider, "Controlling ZIF-8 nano- and microcrystal formation and reactivity through zinc salt variations," *CrystEngComm,* 16(21), 4493-4500, 2014.

[31]. Wang X., Y. Hu, L. Song, W. Xing, H. Lu, P. Lv, G. Jie, "Flame retardancy and thermal degradation mechanism of epoxy resin composites based on a DOPO substituted organophosphorus oligomer," *Polymer,* 51(11), 2435-2445, 2010.

[32]. Liu H., Y. Zhou, Y. Yang, K. Zou, R. Wu, K. Xia, S. Xie, "Synthesis of polyethylenimine/graphene oxide for the adsorption of U(VI) from aqueous solution," *Applied Surface Science*, 471, 88-95, 2019.

[33]. Ding J., S. Tang, X. Chen, M. Ding, J. Kang, R. Wu, Z. Fu, Y. Jin, L. Li, X. Feng, R. Wang, C. Xia, "Introduction of benzotriazole into graphene oxide for highly selective coadsorption of An and Ln: Facile synthesis and theoretical study," *Chemical Engineering Journal,* 344, 594-603, 2018.

[34]. Chen X., Y. Ma, S. Liu, A. Zhang, W. Liu, S. Huang, "A tannic acid-based intumescent flame retardant for improving flame retardancy of epoxy composites," *Advanced Industrial and Engineering Polymer Research,* 8(1), 48-62, 2025.

[35]. Ahmed I., R. Biswas, R. Sharma, V. Burman, K.K. Haldar, "Access to carbon nanofiber composite hydrated cobalt phosphate nanostructure as an efficient catalyst for the hydrogen evolution reaction," *Frontiers in Chemistry,* 11, 1129133, 2023.

[36]. Jadhav AJ H.C., Pandit AB, Pinjari DV, "Intensification of Synthesis of Crystalline Zinc Phosphate ($Zn_3(PO_4)_2$ Nanopowder: Advantage of Sonochemical Method Over Conventional Method," *Austin Chemical Engineering*, 3(2), 1028, 2016.

[37]. Wang H., X. Li, F. Su, J. Xie, Y. Xin, W. Zhang, C. Liu, D. Yao, Y. Zheng, "Core-Shell ZIF67@ZIF8 Modified with Phytic Acid as an Effective Flame Retardant for Improving the Fire Safety of Epoxy Resins," *ACS Omega,* 7(25), 21664-21674, 2022.

THÔNG TIN TÁC GIẢ

Nguyễn Hồng Thắm[1], Hắc Thị Nhung[1,3], Trương Công Doanh[2], Trần Đức Long[4], Hồ Thị Oanh[1], Đoàn Tiến Đạt[1,3], Nguyễn Đức Tuyển[1], Vũ Minh Tân[2], Hoàng Mai Hà[1,3]

[1]Viện Hóa học, Viện Hàn lâm Khoa học và Công nghệ Việt Nam

[2]Trường Đại học Công nghiệp Hà Nội

[3]Học Viện Khoa học và Công nghệ, Viện Hàn lâm Khoa học và Công nghệ Việt Nam

[4]Trường Đại học Sư phạm Hà Nội